



# **Parameters and Depth of Penetration of Barkhausen Noise Analysis**

**by Douglas J. Strand**

**ARL-TR-5159**

**April 2010**

## **NOTICES**

### **Disclaimers**

The findings in this report are not to be construed as an official Department of the Army position unless so designated by other authorized documents.

Citation of manufacturer's or trade names does not constitute an official endorsement or approval of the use thereof.

Destroy this report when it is no longer needed. Do not return it to the originator.

# **Army Research Laboratory**

Aberdeen Proving Ground, MD 21005-5069

---

**ARL-TR-5159****April 2010**

---

## **Parameters and Depth of Penetration of Barkhausen Noise Analysis**

**Douglas J. Strand**

**Weapons and Materials Research Directorate, ARL**

REPORT DOCUMENTATION PAGE				Form Approved OMB No. 0704-0188	
<p>Public reporting burden for this collection of information is estimated to average 1 hour per response, including the time for reviewing instructions, searching existing data sources, gathering and maintaining the data needed, and completing and reviewing the collection information. Send comments regarding this burden estimate or any other aspect of this collection of information, including suggestions for reducing the burden, to Department of Defense, Washington Headquarters Services, Directorate for Information Operations and Reports (0704-0188), 1215 Jefferson Davis Highway, Suite 1204, Arlington, VA 22202-4302. Respondents should be aware that notwithstanding any other provision of law, no person shall be subject to any penalty for failing to comply with a collection of information if it does not display a currently valid OMB control number.</p> <p><b>PLEASE DO NOT RETURN YOUR FORM TO THE ABOVE ADDRESS.</b></p>					
1. REPORT DATE (DD-MM-YYYY)		2. REPORT TYPE		3. DATES COVERED (From - To)	
April 2010		Final		November 2008–September 2009	
4. TITLE AND SUBTITLE Parameters and Depth of Penetration of Barkhausen Noise Analysis				5a. CONTRACT NUMBER	
				5b. GRANT NUMBER	
				5c. PROGRAM ELEMENT NUMBER	
6. AUTHOR(S) Douglas J. Strand				5d. PROJECT NUMBER	
				5e. TASK NUMBER	
				5f. WORK UNIT NUMBER	
7. PERFORMING ORGANIZATION NAME(S) AND ADDRESS(ES) U.S. Army Research Laboratory ATTN: RDRL-WMM-D Aberdeen Proving Ground, MD 21005-5069				8. PERFORMING ORGANIZATION REPORT NUMBER ARL-TR-5159	
9. SPONSORING/MONITORING AGENCY NAME(S) AND ADDRESS(ES)				10. SPONSOR/MONITOR'S ACRONYM(S)	
				11. SPONSOR/MONITOR'S REPORT NUMBER(S)	
12. DISTRIBUTION/AVAILABILITY STATEMENT Approved for public release; distribution is unlimited.					
13. SUPPLEMENTARY NOTES					
14. ABSTRACT The Barkhausen noise analysis (BNA) method is based on a kind of “noise” generated by domain wall movements in ferromagnetic solid materials that exhibit hysteresis. These movements create flips which, in turn, create very small discontinuities along the hysteresis curve. The parameters that affect this Barkhausen noise are examined in this report together with the depth of penetration of the BNA method.					
15. SUBJECT TERMS Barkhausen noise analysis, ferromagnetism, hysteresis					
16. SECURITY CLASSIFICATION OF:			17. LIMITATION OF ABSTRACT	18. NUMBER OF PAGES	19a. NAME OF RESPONSIBLE PERSON
a. REPORT	b. ABSTRACT	c. THIS PAGE			Douglas J. Strand
Unclassified	Unclassified	Unclassified	UU	18	19b. TELEPHONE NUMBER (Include area code) 410-306-0827

---

## Contents

---

<b>1. Introduction</b>	<b>1</b>
<b>2. Theory</b>	<b>2</b>
<b>3. Experimental</b>	<b>4</b>
<b>4. Results</b>	<b>6</b>
<b>5. Discussion</b>	<b>7</b>
<b>6. Conclusions</b>	<b>8</b>
<b>7. References</b>	<b>9</b>
<b>Distribution List</b>	<b>10</b>

INTENTIONALLY LEFT BLANK.

---

## 1. Introduction

---

The Barkhausen effect is the result of the motions of ferromagnetic domains and domain walls called Bloch walls. The mechanics of how these walls are formed and how they adjust is based on the fact that everything tends to its lowest energy state. There are four energies involved in the process. A theoretical examination of the Barkhausen effect is replete with these four terms which are defined as follows:

1. **Exchange energy** is the energy due to the interaction of two spin states.
2. **Magnetostatic energy** is the energy of the magnetic field of a magnet; i.e., the energy associated with a permanent magnet.
3. **Anisotropic energy** is the excess energy required to magnetize a crystal in a hard, as compared to an easy direction. (There are three “easy” directions which are along the defined crystal axes. A diagonal, planar direction is called “medium” and a diagonal, non-planar direction is called “hard.”)
4. **Magnetostrictive energy** is the energy created by a strain on the material ( $I$ ).

Domain motion is governed by the struggle to minimize these four energies.

The following is a list of the conditions under which the four energies are minimized:

1. **Exchange energy**: When all atomic dipole moments are parallel, this energy is minimized.
2. **Magnetostatic energy**: When the integral of  $1/2\mu H^2$  overall space is minimized, this energy is minimized.  $H$  is the external field produced by the magnetic material.
3. **Anisotropic energy**: When the magnetization is along any easy direction, this energy is minimized.
4. **Magnetostrictive energy**: When the material is oriented in such a way that changes in its dimensions are along the magnetization axis, this energy is minimized (2).

An applied magnetic field will upset the minimizing balance of these four fundamental energies. The Barkhausen effect occurs during the process of restoring this balance.

---

## 2. Theory

---

Aside from destroying a sample, destructive testing has the disadvantage of only allowing a very small portion of a lot of material to be inspected. With nondestructive evaluation, 100% of the samples can be tested without damaging even one specimen.

The major nondestructive testing techniques utilized by the U.S. Army Research Laboratory (ARL) at Aberdeen Proving Ground, MD, and in the field are acoustic emissions, electromagnetic, liquid penetrant, magnetic particle, radiography, and ultrasonic. The effect is an electromagnetic technique.

In its simplest form, the Barkhausen effect states that the hysteresis loop of a ferromagnetic material is not a smooth curve. There are discontinuities, or jumps, that occur along its path on a microscopic level. Hysteresis occurs because the domain boundaries do not move totally back to their initial positions when the external field is removed (3).

This discontinuous change in magnetization produces a noise-like signal similar to the time derivative of the actual magnetic flux into a coil which has been placed near the material being magnetized (4).

When the applied magnetic field strength exceeds certain threshold values, the domain walls inside the material will move, causing the Barkhausen jumps which are simply discontinuities along the hysteresis curve. Since the middle range of the magnetizing field,  $H$ , causes the steepest slope,  $dH$ , in the hysteresis loop, it is here that these threshold values are most likely to be exceeded and Barkhausen jumps occur (5). Irreversible domain wall boundary motions predominate in the medium field range.

At low field values magnetization increases by reversible boundary displacements, and in the high field range reversible domain rotations predominate (6). The potential barriers caused by dislocations, precipitates, or other obstacles which “pin” the walls are surmounted at mid-range due to the greater change in flux density here. This is why the phenomena at mid-range is irreversible, while at low and high range it is reversible (7).

Microscopically, the domain wall movements are caused by changes in direction of atomic magnetic moments. These moments change their directions by  $90^\circ$  or  $180^\circ$  inside domain walls at the easy (crystal axis) magnetization directions. However, no such changes occur until wall displacements are completed (8). For materials such as iron, the  $\langle 100 \rangle$  lattice directions are the easy directions (9). Domain walls move through a crystal when an applied magnetic field is varied. If the domain wall encounters an inclusion, it is elastically jerked onto it and will stay on top of the inclusion until the magnetic field is further varied; then it will move away from the



inclusion elastically until it reaches an “elastic limit” where it will snap free from the inclusion. These jerks and snaps are what cause an induced voltage pulse in a coil wound on the specimen (10).

Two important formulas arise from the domain wall calculations (11). First, a formula for the effective wall thickness:

$$\delta = 2 \frac{\sqrt{M}}{2K_0} = \frac{\sqrt{2M}}{K_0}, \quad (1)$$

where  $M$  is the particle mass and  $K_0$  comes from the crystalline-anisotropy energy density,  $K_0 \alpha_1^2$ . Second, a formula for the free energy  $\gamma_w$  per unit area of the wall:

$$\gamma_w = f_H = 2K_0 \int_{-\infty}^{+\infty} \cos^2 \phi \, dZ = \sqrt{2MK_0} \int_{-\frac{\pi}{2}}^{+\frac{\pi}{2}} \cos \phi \, d\phi = 2\sqrt{2MK_0}, \quad (2)$$

where  $\phi$  is the meridional angle of cylindrical coordinates and where  $\phi$  is the angle that the magnetic moment makes with an arbitrary initial or standard direction.

There are two pressures on the domain wall which must balance in order for it to be in equilibrium. The first is the pressure due to the magnetic field, and the second is the pressure due to inhomogeneities,  $-\frac{d\gamma_w(Z)}{dZ}$ , where  $\gamma_w(Z)$  is the energy per unit area of a wall “at” (i.e., with its midplane at)  $Z$ . The energy “wells” which create the dynamics of a Barkhausen jump are shown in the simple graphic in figure 1. Thus,  $\gamma_w(Z)$  will be at a minimum, A, at zero field. As the field increases, the wall moves reversibly until it reaches a point of inflection, B, of  $\gamma_w(Z)$ . From here it goes to a position of stable equilibrium, C, by undergoing a finite irreversible displacement. This is a Barkhausen jump (12).

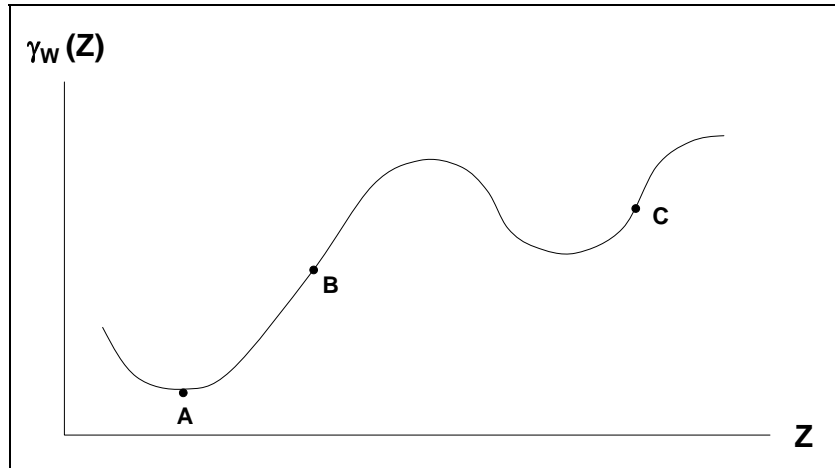


Figure 1. Domain wall energy.

---

### 3. Experimental

---

The Barkhausen noise analysis (BNA) method has been used by both the government, academia and industry to examine grain size, carbon content, applied tension, and plastic deformation. Potentially, it can be used to characterize metallurgical, microstructural, and mechanical parameters.

The Barkhausen noise (BN) threshold, which is the threshold of the background noise, has been determined to be the minimum value of the BN envelope at the magnetic saturation region. As a result of these measurements, the following BN parameters were evaluated: root mean square (RMS) value, frequency spectrum, BN envelope or RMS profile of BN, BN energy or time integral of BN envelope as a function of real sample field, and pulse height distribution of BN.

After analysis of these results, Stupakov et al. (13) proposed an optimized sensor with a controlled waveform to improve the measurement repeatability. This is an integrated BN sensor that combines a single yoke, the field sensor(s) for magnetization control with digital feedback, and the pancake coil of a prototype BNA system.

The BN signal is of a stochastic nature, so that only the average properties are reproducible. Therefore, the point parameters, such as the peak value (position) of the BN envelope or the single frequency component of the BN spectrum, are not generally reliable. There are two ways to handle the BN parameters today: using data averaging over either adjacent points or consequent magnetization cycles. Because of the background noise, the magnetic information is only contained in the tail of the pulse height distribution. After an extensive literature search, there have been no known reports of the successful application of BN jump parameters over the RMS-based values (13).

A Stresscan 500C instrument was used to examine cylindrical steel specimens at several points which are described as high area and low area regions.

The statistical distributions of the Barkhausen noise is known to have distortions. These distortions can be measured by the magneto-optical Kerr effect (MOKE). The light that is reflected from a magnetized surface can change in both polarization and reflectivity. The MOKE is identical to the Faraday effect except that it is a measurement of the reflected light, while the Faraday effect is a measurement of the transmitted light. Both effects result from the off-diagonal components of the dielectric tensor  $\varepsilon$ . The relationship between the electric displacement field,  $D$ , and the electric field,  $E$ , is:  $D = \varepsilon E$ .  $\varepsilon$  is also called the permittivity and is a scalar if the material in question is linear, homogeneous and isotropic, but can be a tensor if the material is anisotropic. Using the MOKE, Pinotti et al. (14) have developed statistical distribution formulas for both a uniform beam and a Gaussian.

A Stresscan 500C was used to examine a cylindrical steel specimen at several points which are described as high area and low area regions.

To examine the distribution of BN signals, nine ferromagnetic specimens were examined at ARL at opposite orientations, 0 and 90°. The collected values are recorded as follows:

Specimen One:			
<u>Front 0</u>	<u>Front 90</u>	<u>Back 0</u>	<u>Back 90</u>
35.5	20.8	15.2	15.2
38.6	53.8	14.9	13.3
80.2	85.5	18.6	13.6
42.5	49.6		
80.5	81.4		
47.2	63.6		
110.0	90.1		
40.2	32.7		
102.0	116.0		

Specimen Six:			
<u>Front 0</u>	<u>Front 90</u>	<u>Back 0</u>	<u>Back 90</u>
69.0	68.4	18.7	18.1
32.7	21.6	17.8	14.6
91.8	75.2	19.5	14.6
41.3	29.9		
91.5	89.0		
45.2	33.4		
92.9	80.8		
43.9	33.0		
46.8	40.0		

Specimen Two:			
<u>Front 0</u>	<u>Front 90</u>	<u>Back 0</u>	<u>Back 90</u>
98.7	98.1	15.2	14.6
39.9	32.4	15.4	13.1
49.0	72.5	15.1	12.1
43.5	27.5		
44.9	51.1		
50.6	44.5		
41.7	57.7		
39.3	25.1		
38.9	38.1		

Specimen Seven:			
<u>Front 0</u>	<u>Front 90</u>	<u>Back 0</u>	<u>Back 90</u>
53.4	61.7	18.5	15.4
35.5	28.4	16.6	17.9
35.4	45.2	18.7	13.5
33.1	33.2		
34.6	38.6		
71.0	63.8		
46.4	52.5		
43.2	50.7		
33.3	36.4		

Specimen Three:			
<u>Front 0</u>	<u>Front 90</u>	<u>Back 0</u>	<u>Back 90</u>
24.2	17.4	15.2	15.6
36.4	59.3	16.2	16.0
46.9	42.4	19.1	19.0
43.5	69.5		
45.0	30.4		
44.1	50.4		
36.6	32.4		
33.7	23.6		
34.8	52.8		

Specimen Eight:			
<u>Front 0</u>	<u>Front 90</u>	<u>Back 0</u>	<u>Back 90</u>
24.4	31.4	17.6	15.7
38.4	35.4	16.8	15.7
82.0	68.6	21.7	17.6
49.8	52.5		
39.0	42.1		
45.8	54.0		
41.2	43.6		
33.5	32.7		
66.4	79.4		

Specimen Four:				Specimen Nine:			
<u>Front 0</u>	<u>Front 90</u>	<u>Back 0</u>	<u>Back 90</u>	<u>Front 0</u>	<u>Front 90</u>	<u>Back 0</u>	<u>Back 90</u>
55.2	31.6	11.6	10.2	72.6	72.3	14.7	14.7
40.2	23.6	9.4	10.9	39.4	22.0	14.2	14.1
111.0	86.3	19.1	15.7	74.2	73.5	15.9	11.6
59.5	42.6			41.8	36.4		
84.7	82.0			69.3	76.5	maximum location	
44.7	27.6			38.3	31.5		
73.9	68.9			72.8	70.3		
36.7	24.3			35.1	37.6		
81.1	82.0			34.6	30.2		

Specimen Five:

<u>Front 0</u>	<u>Front 90</u>	<u>Back 0</u>	<u>Back 90</u>
42.0	31.9	15.3	12.6
74.4	73.7	15.4	15.4
37.5	27.4	17.6	15.5
72.5	61.7		
33.5	21.9		
77.4	72.9		
42.1	22.0		
60.7	57.6		
44.5	37.4		

## 4. Results

The strength of a BNA signal will decrease with increasing depth. The data for steel in table 1 shows this decrease in strength. The BNA signal decreases by a much greater percentage near the surface than it does at greater depths. Whether the signals are of a large magnitude or a small magnitude, decreases in the BNA signal decreased by 70% at depths from 0.07 to 0.20 mm as compared to depths from 0.02 to 0.07 mm.

Table 1. Specimen results.

Sensor (S/N 2483) With MAGN = 50		
Depth Setting (mm)	High Area (MP)	Low Area (MP)
0.02	258	65.0
0.07	140	34.4
0.20	58.5	12.6

The BN signals from the nine ferromagnetic specimens indicate that there are indeed variations in the signal strengths that must be accounted for by a statistical method. The initial stages of this work have been accomplished in this report by examining the stable parameters of the Barkhausen noise analysis method.

---

## 5. Discussion

---

The appearances of BN depend on the kind of ferromagnetic specimen being studied, the character of quenched in defects, the external field driving rate, thermal effects, the strength of the demagnetization fields, and other experimental parameters. There are several theoretical approaches to the explanation of BN. First is the domain wall (DW) motion approach. The Langevin equation has been used with this approach and ultrathin ferromagnetic films have been investigated using it. The self-organized criticality (SOC) approach is the second approach. This approach has been used with the Jensen, Christensen, and Fogedby (JCF) type of analysis which is a statistical characterization of the observed BN. Third, is the fractal time signal approach and fourth, the O'Brien and Weissman approach which basically refutes the SOC approach. In this approach, the  $1/f$  noise and power-law distributions are not necessarily evidence of SOC, but are rather the consequences of scaling properties of quenched disorder in material. The fifth and final approach is the Urbach et al. (15) approach which exploits the concept of rough-surfaces growth to describe the DW motion, with the result that long-range demagnetization fields strongly affect the character of the BN.

It has been found that the BN elementary signal's (BNES) probability distribution function is a generalized homogeneous function (GHF) which enables us to re-derive all scaling relations in the framework of standard critical phenomena (14).

The BNES can be described mathematically by the two component equation:

$$f(t') = \begin{cases} Ct'^{\gamma-1}g(t'/T), & t' > 0 \\ 0, & t' \leq 0 \end{cases}, \quad (3)$$

where  $C$  is a proportionality constant,  $\gamma$  is the corresponding signal exponent, and  $g(t'/T)$  is some function which is close to one for small values of the argument and decreases rapidly to 0 as the values of  $t'/T$  increase. Here,  $t'$  is the time measured from the beginning of the elementary signal and  $T$  can be thought of as the duration of the elementary signal (16, 17).

---

## **6. Conclusions**

---

BNA is primarily a surface test method due to the attenuation of its signal by eddy current shielding effects. For greater depth of penetration testing the magneto-acoustic emission (MAE) method, the ultrasonic method, or radiography method should be used. An analysis of the data shows that the BNA method is more reliable at greater depths than previous studies have shown. This data was collected for steel and the result will be tested for any metal matrix composite materials that may contain ferrous elements and for any other ferrous-like composite materials.

---

## 7. References

---

1. Plonus, M. A. *Applied Electromagnetics*; McGraw-Hill, Inc.: New York, 1978, 361–367.
2. Ibid., p 361.
3. Halliday, D.; Resnick, R. *Fundamentals of Physics*; John Wiley and Sons, Inc.: New York, 1970, 621.
4. Sundstrom, O.; Torronen, K. *Materials Evaluation* **February 1979**, 37, 51.
5. Weinstock, H.; Erber, T.; Nisenoff, M. *Phys. Rev. B.* **1985**, 31, 1535.
6. Leep, R. W. *Op. Cit.*, 440–441.
7. Weinstock, H. *Op. Cit.*, 1536.
8. Brown, W. F., Jr. *Magnetostatic Principles in Ferromagnetism*; Interscience Publishers, Inc.: New York, 1962, p 167.
9. Sundstrom, O.; Torronen, K. *Op. Cit.*, 51.
10. Pasley, R. L. *Materials Evaluation* **July 1970**, 28, 158.
11. Brown, W. F., Jr. *Op. Cit.*, 158.
12. Ibid., p. 165.
13. Stupakov, O.; Pal'a, J.; Takagi, T.; Uchimoto, T. Governing Conditions of Repeatable Barkhausen Noise Response. *J. Magn. Magn. Mater.* 2009, doi: 10.1016/j.jmmm.2009.04.065, article in press.
14. Pinotti, E.; Brenna, M.; Puppini, E. Distributions of the Statistical Distribution of Barkhausen Noise Measured by The Magneto-Optical Kerr Effect. *J. Magn. Magn. Mater.* **2008**, 320, 1651–1656.
15. Urbach, J. S.; Madison, R. C.; Market, J. T. *Phys. Rev. Lett.* **1995**, 75, 276.
16. Spasojević, D.; Bukvić, S.; Milošević, S.; Stanley, H. E. *Barkhausen Noise: Elementary Signals, Power Laws, and Scaling Relations, Physical Review E* **September 1996**, 54 (3), 2531–2532.
17. Ibid., p 2537.

NO. OF  
COPIES ORGANIZATION

1 DEFENSE TECHNICAL  
 (PDF INFORMATION CTR  
 only) DTIC OCA  
 8725 JOHN J KINGMAN RD  
 STE 0944  
 FORT BELVOIR VA 22060-6218

1 DIRECTOR  
 US ARMY RESEARCH LAB  
 IMNE ALC HRR  
 2800 POWDER MILL RD  
 ADELPHI MD 20783-1197

1 DIRECTOR  
 US ARMY RESEARCH LAB  
 RDRL CIM L  
 2800 POWDER MILL RD  
 ADELPHI MD 20783-1197

1 DIRECTOR  
 US ARMY RESEARCH LAB  
 RDRL CIM P  
 2800 POWDER MILL RD  
 ADELPHI MD 20783-1197

1 DIRECTOR  
 US ARMY RESEARCH LAB  
 RDRL D  
 2800 POWDER MILL RD  
 ADELPHI MD 20783-1197

ABERDEEN PROVING GROUND

1 DIR USARL  
 RDRL CIM G (BLDG 4600)



NO. OF  
COPIES ORGANIZATION

ABERDEEN PROVING GROUND

21    DIR USARL  
      RDRL WMM D  
      E CHIN  
      D STRAND (20 CPS)

INTENTIONALLY LEFT BLANK.